

MA1 Project

*Rapid Design of Sensorized Interfaces for Upper Arm
Exoskeletons: Benchmarked on EMG Sensors*

Author

Manar MAHMALJI

Supervisors

ing. Kevin LANGLOIS
Prof. dr. ir. Tom VERSTRATEN

August 2021

Contents

1 Acknowledgments	3
2 Abstract	3
3 Introduction	4
3.1 General Background	4
3.2 Scope of Study	5
3.3 State-of-the-Art	8
3.4 Goal Statement	9
4 Preliminary Setup of 3D Scans	11
4.1 Setup for Stretched Arms	11
4.1.1 Consistency of Elbow Cuts	13
4.2 Setup for Flexed Arms	13
5 Circumference and Area Measurement	14
5.1 MATLAB Algorithm	14
5.1.1 Finding Section Points	15
5.1.2 Curve-fitting	16
5.2 Validation with CAD Software	18
5.3 Robustness	19
6 Shoulder Identification for Stretched Arms	20
6.1 Theoretical Framework and Scanning Guidelines	20
6.2 MATLAB Algorithm	21
6.2.1 Humerus Length Comparison with Body Length	22
7 Shoulder and Elbow Identification for Flexed Arms	23
7.1 Theoretical Framework	23
7.2 MATLAB Algorithm	24

7.2.1	Shoulder Identification	24
7.2.2	Elbow Identification	25
8	Benchmarking: Biceps Brachii Identification	27
9	Conclusions and Future Work	28
10	Annex	30
10.1	Right Views of All Stretched Arm Scans	30
10.2	Right Views of All Flexed Arm Scans	31
10.3	Cubic Spline Fitting Method	32
11	Bibliography	32

1 Acknowledgments

I would like to thank the supervisors for accepting me into this MA1 project. Particularly, I wish to genuinely express my gratitude for Kevin Langlois for his unwavering support , especially in the last weeks before the deadline and his constructive feedback that challenged me to think more critically in every meeting we had.

2 Abstract

Exoskeletons, with their many shapes and uses, have been a fertile ground for research since the dawn of the 21st century. One novel area of research is the development of a sensorized and customized interface within an exoskeleton for the sake of improving the assistance it provides as well as its wearability. Therefore, in the aim of facilitating the integration of sensors into upper arm exoskeletons, this study proposes a MATLAB algorithm that takes a 3D scan of a healthy arm and outputs, without markers, certain upper arm measurements that makes the design process less time-consuming and sets an additional iteration in the effort of making the design process of an exoskeleton more data-driven.

Keywords: [EMG](#), [3D scanning](#), [upper arm exoskeleton](#), [sensorized and customized interface](#), [biceps brachii identification](#), [shoulder and elbow identification](#), [circumference and area measurement](#)

3 Introduction

3.1 General Background

Exoskeletons are wearable robotic devices that have been developed into several fields depending on their application, which makes them possible to divide into three different categories: exoskeletons for human performance augmentation, assistive devices for individuals with disabilities and therapeutic exoskeletons for rehabilitation [1]. According to the World Health Organization, it is estimated that 74% of years lived with disability (YLDs) in the world are the result of health conditions for which rehabilitation may be beneficial. Moreover, 15% of all YLDs are caused by health conditions associated with severe levels of disability. On the other hand, the density of skilled rehabilitation practitioners is less than 10 for every 1 million people in many low- and middle-income countries. Therefore, the number of occupational therapists, physiotherapists, physical medicine and rehabilitation doctors, and prosthetists and orthotists is far from what is required [2]. For this reason, the development of clinical human-machine systems such as powered robotic exoskeletons and other wearable devices has advanced considerably in the last decade. After injuries of a body part or surgery, a rehabilitation process is necessary to regain as much dexterity back as possible. For example, rehabilitation can be required to prevent agglutination or adhesion of the involved tissue. After long periods of being unable to use the part, it may also be required to relearn basic movement [3]. Therefore, although initially expensive, exoskeletons provide therapists with the possibility to save time, physical effort, and help more patients. Some ways in which exoskeletons can help are: monitoring and controlling movement speed, direction, amplitude, joint coordination patterns, and controlled perturbations; providing weight support with minimal exertion; and offering the potential for more reliable, standardised tests and goniometry measure [4].

Some examples from the commercially available medical exoskeletons are given below:



(a)



(b)



(c)

Figure 1:

(a)

Phoenix is a 23 lbs exoskeleton that has motors that control hip and knee movements. Its average walking speed is 1.1 miles/hour, and its battery life allows for approximately 4 hours of continuous walking. It's meant for use in the clinic and community [5]

(b)

HAL is used in clinic, and it uses a technology that senses electrical signals sent from brain to the muscles and initiates the required movement for the patient. This may be especially useful in early gait rehabilitation to establish stronger brain-muscle connections. If no signals are detected (e.g. paraplegia) then the robot has an automated gait pattern that it puts the person through. It weighs 23kg, it can lift a max weight of 73kg, and it has a battery life of 40 minutes to 2 hours [6]

(c)

The eksoUE is a passive shoulder and elbow support exoskeleton for medical rehabilitation. It is in many ways similar to the eksoVest, one of the first spring-activated industrial shoulder-support exoskeleton [7]

3.2 Scope of Study

On the other hand, ElectroMyoGraphy(EMG) sensors are used in the aim of improving the response and assistance of the exoskeleton, particularly for patients with limited to almost null body part mobility(eg. Tetraplegia). ElectroMyoGraphy is the sensing and recording of electrical waveforms that result from muscle activity. Each muscle is comprised of many muscle motor units, which are comprised of many cells, and are connected to many motoneurons, thus a seemingly simple muscle contraction will correspond to a complex overall MAP- Muscle Action Potential- waveform. An electrode properly positioned with respect to the muscle can record these MAP waveforms [13]. Since the action potential is an electrical signal and the skin is a moderately conductive tissue, as well as the tissue between the muscle fibres and the skin, it is possible to measure it by placing a metal surface or even a conductive material directly over the skin, namely the EMG electrode. This is called surface EMG [14] Another method for measuring

the action potential is the intramuscular method, where needle based electrodes are inserted through the skin into the muscle of interest. Intramuscular EMG is the preferred method when measuring small muscles, particularly those surrounded by large muscles which may prevent accurate recording of the signal of interest or when attempting to measure only a few motor units. Surface EMG is preferred when studying large muscles, especially those near the surface and with few large muscles nearby. An added advantage of surface EMG is that the electrodes are adhered to the skin surface, thus piercing of the skin is not required [13].



Figure 2: EMG Electrodes

Methods of Utilizing EMG Signals:

According to a detailed study (13), electromyography can be used in many ways for various applications, with various techniques and concerns corresponding to each new application.

- First Method: **Sense and emulate/amplify**

Here, Electromyography is used to sense the activity of a muscle and the myoelectric signal is processed in order to determine an activation magnitude as a function of time. This magnitude is then used to determine a target force, position, or motion of a worn mechanical device emulating, or actually worn over the same limb. In this method, the myoelectric signal is interpreted in order to determine a discrete magnitude, not a target threshold value[13]. This method is used for example, in controlling the HAL exoskeleton shown in Figure 1-(b).

- Second Method: **Sense and interpret, proportional**

Similar to method one, EMG is used to determine activation level of a muscle as a function

of time. Rather than interpreting the signal in order to control a local device and directly emulate the limb being sensed, this method interprets the signal in order to provide input to another device, either locally or remotely. A good example of this is shown in study [15] where EMG signals from one hand were used to control an upper limb exoskeleton mounted on the second hand.

- Third Method: **Sense and interpret, threshold**

A myoelectric signal is read, processed, and compared to a predetermined threshold value. When that value is reached, a condition is considered satisfied. Rather than interpreting a signal to determine a curvilinear magnitude with respect to time, this application is more similar to an on-off switch. This method is believed to cause less fatigue for users than the proportional control in method 2 because with the threshold value technique, the controlling muscle is not required to maintain a consistent activation level to maintain the device state[13].

As seen above, one of the main properties of EMG is the proportional myoelectric control system which utilizes electromyography (EMG) signals to proportionally activate the corresponding joint actuator(s) inside an exoskeleton. Much literature about setting up EMG control circuit as well as measurement procedure can be found in the studies [14], [16] and [17].

Why is EMG technology important to integrate within the exoskeleton-human interface?

Human-machine interaction can be implemented by using force and/or pressure sensors. One problem of the human-machine interaction is that the force sensors integrated into the construction do not distinguish between forces exerted by the user and external forces. During contact with the environment, it becomes impossible to recognize the user's intention. This intention can be detected by acquiring the physiological muscle signals by the EMG sensors [3]. Furthermore, the detection of muscle activity enables patients with slight body part mobility to utilize the integrated exoskeleton. In conclusion, the EMG sensors enhance the exoskeleton's control efficiency and provide a particularly intuitive and convenient interface, whereas simultaneously, the force and/or pressure sensors monitor the interaction forces between the user

and the exoskeleton, ensuring the user's safety and comfort.

3.3 State-of-the-Art

EMG Electrodes Integration Constraints:

- **Accuracy and Processing of Measurements**

EMG signals aren't stable over time and it is difficult to obtain the same EMG signal for the same motion, even with the same person, since they depend on a variety of factors such as the placement of the sensors, fatigue of the muscles and sweat. Also, because there are many muscles involved in every joint motion, it is not easy to predict with accuracy to which motion each signal corresponds [18], [19]. Furthermore, the density of the human muscles is high resulting the muscle signals to superimpose at the electrodes [3]. Even after the Blind source separation- study [3]-the signals are not separated ideally and it is not entirely possible to have muscle signal decomposition for the different degrees of freedom

- **Selection and Localization of Muscles**

The muscle selection and sensor placement is a difficult problem. The human hand, for example, has up to 40 muscles, and some of them are also split into muscle compartments [3]. The selection of muscles to measure and electrode placement is critical to effective use of EMG for exoskeleton and machine control, particularly if a worn device is intended to perform such complex tasks as interpreting a wearer's intent. A selection of muscles and sensor locations must maximize signal strength, and minimize noise/crosstalk [13]. Literature on the locations of certain muscles for performing EMG can be found on SENIAM (surface ElectroMyoGraphy for the Non-Invasive Assessment of Muscles)- [20]

- **Motion Artifacts**

Motion artefacts produce the largest disturbances in the measured EMG signals. A common phenomenon that contributes to the motion artefact is the change in relative position of electrodes to the skin[21]. It influences the size of the contact surface, introduces skin deformation, and produces changes on the interface layer due to changes in conductive gel thickness/amount or the amount of sweat, which in turn results in electrical

coupling. Consequently, there is significant electrical signal distortion. Movement artefacts produced during normal activities, including locomotion, can have amplitudes that are an order of magnitude larger than signals produced by brain activity . Motion artefacts are non-stationary, time-varying electrical signals [21]. Hence, to avoid them any electrode placement should not be overly invasive, cause discomfort, and can not obstruct proper use of the device [13]

Solutions and Previous Projects:

These competing constraints often make EMG sensor placement a difficult task to fulfil. Nonetheless, there are some companies and research groups that achieved remarkable results, some of which are shown in figure 3.

3.4 Goal Statement

EMG-based controllers for exoskeletons have proven their efficacy to provide the user with natural control over the wearable robot. It is no surprise that this technology is seeing a lot of interest from companies and exoskeleton developers across the world. However, the main constraint of using such technologies is the location of the electrodes, that need to be precisely determined, and often manually placed by an expert. Therefore, the goal of this study is to develop a framework that can facilitate the development of customized, and sensorized interfaces for exoskeletons. The framework consists of 3D scanning of the upper arm and a MATLAB software algorithm is developed so that it can semi-automatically identify regions and landmarks of interest to the designer, namely the area and circumference of any crossection along the orthonormal axes, the shoulder and elbow joints approximations, humerus length ,and finally as a use case, the algorithm tries to estimate the EMG electrodes locations for the Biceps Brachii. This software can be used for rapid prototyping of sensorized interfaces. This will facilitate the commercialization of such exoskeletons as as the process of building them will become semi-automated and customized to each user's body shape.

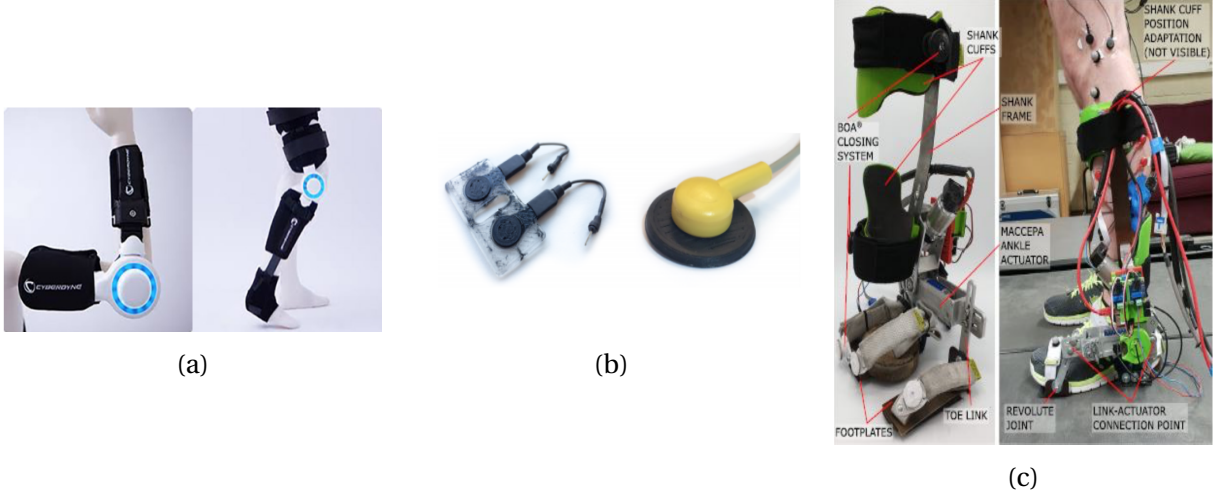


Figure 3:

(a)

The most remarkable and unique results for EMG controlled exoskeletons were achieved by the Japanese company Cyberdyne. What follows is quoted from their website “When a person moves his or her body, the brain sends various signals to muscles via nerves. At that time, the signals leak out on the skin surface as BES. HAL for Well-being Single Joint Type reads the wearer’s BES and actuates its small power unit. Therefore, it is able to perform assistance in alignment with the wearer’s “will” and consequently gives the vivid feeling “I could move my joint by myself” to the wearer ” [6]

(b)

In the study [23], it was proven that it was possible to 3D print a working EMG sensor, and an algorithm was developed which detected the possible locations where the deformations could appear in lower limb muscles, hence enabling the design of an optimised orthosis in which the places for EMG electrodes are known. This will certainly pose a challenge later on when the orthosis is under trial in terms of keeping the electrode in contact with skin as well as reducing motion artefacts.

(c)

Other solutions include modifying/trimming the orthosis geometry so that it doesn't touch the EMG electrodes. This can be seen in figure 9 below from the study [30]. It can be seen that the electrodes can be accidentally dislodged during movement. Furthermore, reducing surface area to make space for EMG electrodes may be at the expense of increasing local pressures on the limb.

4 Preliminary Setup of 3D Scans

This study was performed with 9 scans of stretched arms and 2 scans of flexed arms. All the 3D scans were imported as *.stl* files, but as they are raw scan, some processing must be done to extract the upper arm. The processing was done with the mesh editing software *Autodesk Meshmixer*, version 3.5.474 . Special care was taken to make the process as generalized as possible.

4.1 Setup for Stretched Arms

The right views of all the scans are present in the Annex. The demonstrative procedures in this section were done on sample 8, but the same applies for all samples.

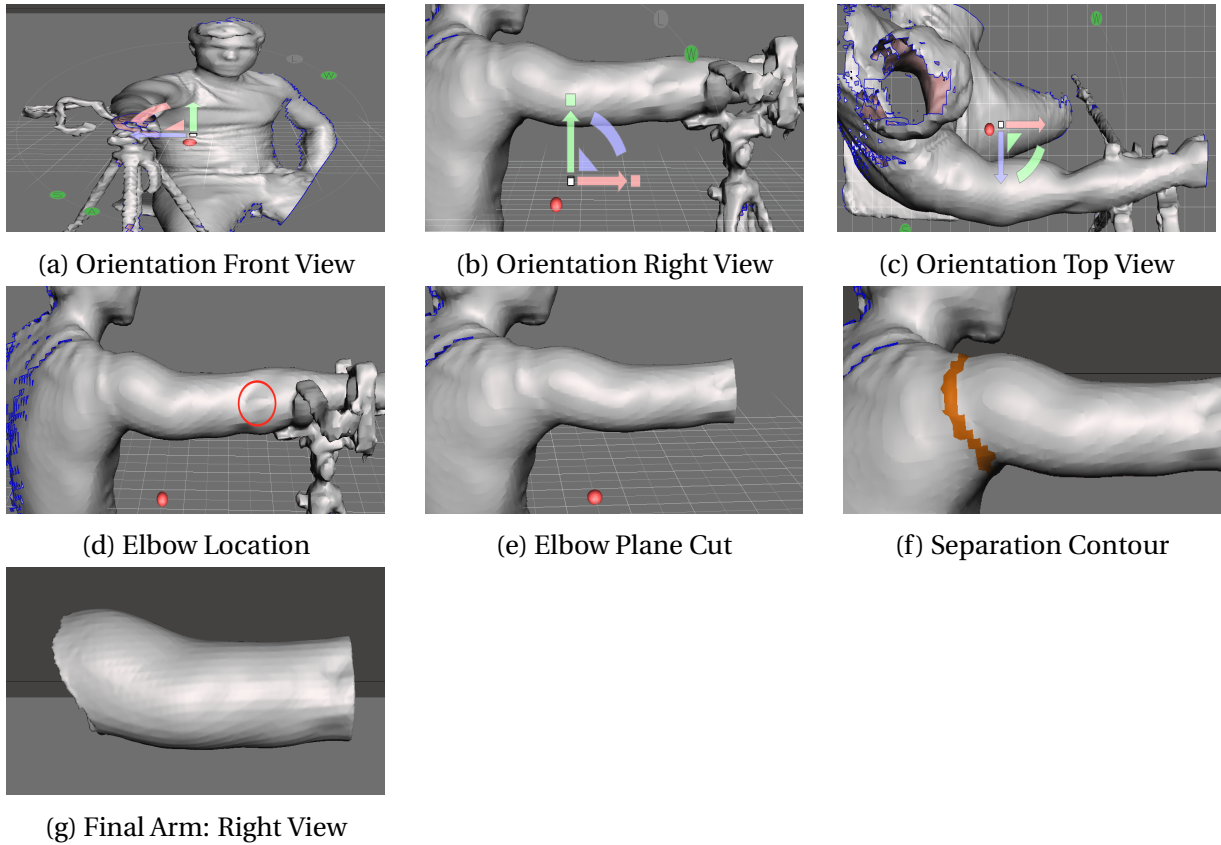


Figure 4: Separation procedures of upper arm from raw 3D scans of stretched arm in Meshmixer

- **Units:** the first step is to make sure that the units inside the Analysis tab are in mm and are logical.

Ex: $x=0.653$ mm should be edited to be 653 mm

- **Orientation:** using the transform tool in the edit tab, set the coordinate space into world frame and align the subject's body along the z-axis(green arrow) as shown in figure 4-(a) . Then, align the upper arm along the x-axis (red arrow) as shown in figures 4-(b) and 4-(c) The arm should be aligned with the x-axis from right and top views.
- **Plane Cut at Elbow:** using the plane cut tool in the edit tab, align the plane so that it is perpendicular to the plane of the page by making a 90 degrees rotation, then cut the arm at the center of the elbow. The elbow is either determined by the small protrusion between the upper and fore arms. Figures 4-(d) and 4-(e) show an approximate position of the elbow and the obtained arm after the cut, respectively.
- **Separation of Upper Arm From Body** using the brush tool in the select tab, a closed contour is drawn along the line approximately separating the Deltoid muscle from the Trapezius muscle.

By looking at the shoulder muscles in figure 5, it can be seen that this line is approximately along the U-shaped concavity between the Trapezius and Deltoid muscles. This concavity, marked with the red ellipse , is not clear for all samples due to the reasons discussed in section 6.1, therefore, this cut is only done on certain samples that are mentioned in section 6.1 which are samples 1,3,6,7, and 8. However, for the remaining samples that will only be used in circumference and area measurement, this cut is acceptable at any line around the Deltoid muscle or even a plane cut can be done as in the previous step.

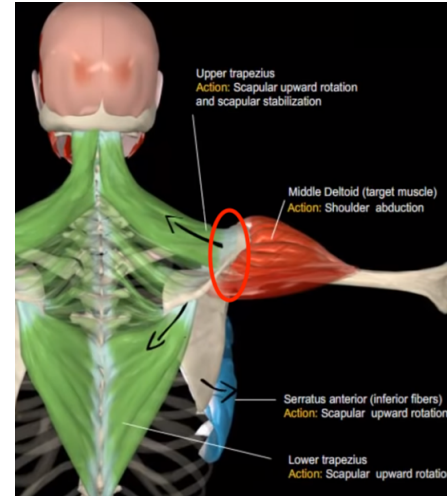


Figure 5: Shoulder Muscles[40]

Having drawn the selected line, the separate option in the edit menu of the select menu is used. This enables to use the separate shells tool in the edit menu to get a separate shell of the upper arm. Finally, by choosing the shell of the upper arm, the make solid tool is used to fill or repair any holes and then it is ready to be exported as *.stl* file. Figures 4-(f) and 4-(e) show the drawn contour and the final result of the scan, respectively.

4.1.1 Consistency of Elbow Cuts

For the samples referenced in section 6.1, it is imperative to guarantee the consistency of elbow cuts as the scans will be processed to get the biceps brachii and calculate the humerus length; therefore, the elbow position should be as consistent for all the scans as possible. For this reason, the Plane Cut at Elbow was done with one plane, as shown in figure 7, for samples 1,3,6,7, and 8 ordered from up to down.

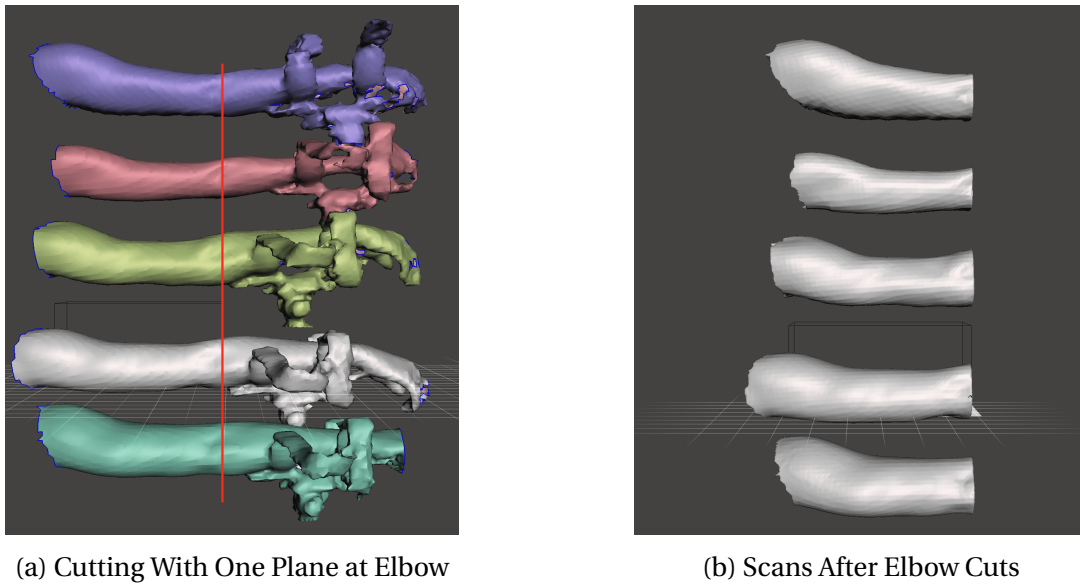
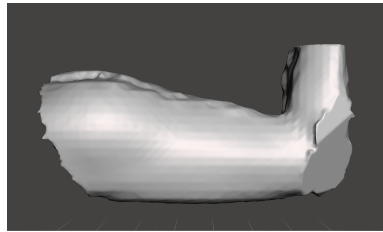


Figure 6: Consistent Cutting for the Scans Referenced in Section 6.1

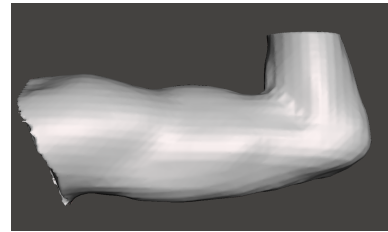
4.2 Setup for Flexed Arms

The number of scans with flexed arms for this study is 2. The same procedures applied for stretched arms in **Units**, **Orientation**, and **Separation of Upper Arm From Body** hold for the flexed arm. The difference lies in **Plane Cut at Elbow**. For flexed arms, the cut is done at any

point slightly above the elbow with a plane parallel to the XY plane. The final results are shown in figure 5



(a) scan(1)



(b) scan(2)

Figure 7: Separation of upper arm from 3D scans of flexed arm in Meshmixer. The same procedures for stretched arms hold for the flexed arms except that there is no cutting at elbow, rather slightly above it.

5 Circumference and Area Measurement

The circumference and area measurement for segments/sections along the upper arm or any body part are crucial for any exoskeleton design process. As there are users with various body sizes, the design process for each individual should be tackled separately. Thus, by finding the area and circumference along the upper arm, the design process becomes more customizable and less time-consuming.

5.1 MATLAB Algorithm

Demonstrative figures are taken from a random sample. The algorithm is equally applicable to all samples.

5.1.1 Finding Section Points

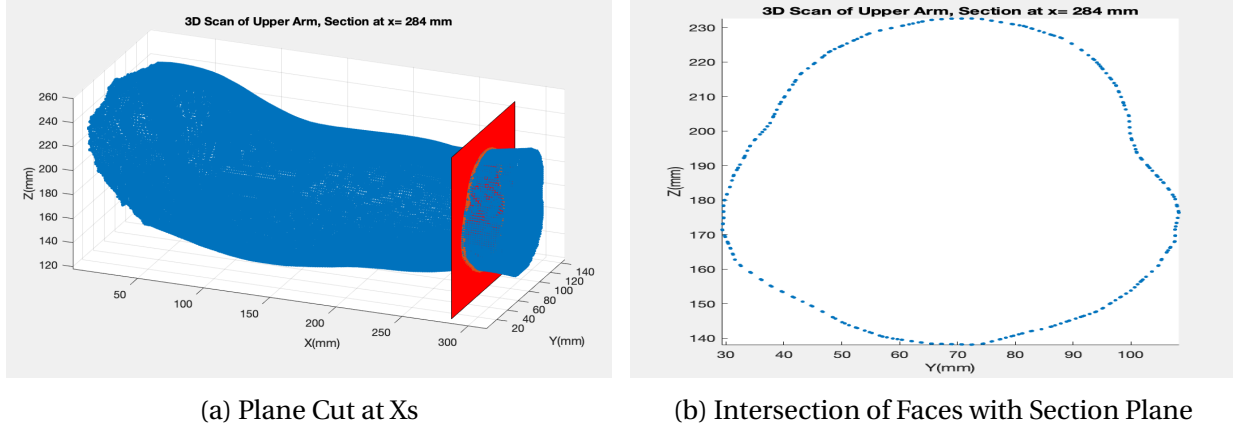


Figure 8: Finding Section Points

Following the directions in section 4.1, the exported upper arm has its elbow cross section perpendicular to the x-axis with the X_{max} being from the elbow's side. This orientation is always considered fixed for any upper arm exported to the algorithm. Using the built-in function *stlread*, the final scan is read into MATLAB and stored as two matrices: *faces* and *vertices*. As the above orientation is always maintained, it is always possible to cut the arm with sections along the x-axis as shown in figure 8-(a). Denote by X_s the the x-coordinate that is far by a certain offset value from X_{max} , namely the elbow point. The faces of the imported mesh are triangular, but the procedures are the same for quads. The proposed algorithm operates as follows to find the resulting section at X_s :

1. For each face, calculate the relative distance between each face's vertex and the section plane. If the all the vertices have the same sign, then the plane doesn't intersect the face.
2. Otherwise, if they have different signs, there is intersection. In this case, two edges are obtained by connecting the vertices that have different signs. Each edge intersects the plane with a point.
3. Denoting by V_1 and V_2 the vertices of an edge, a scaling factor is defined: $t = \frac{X_{V1}-X_s}{X_{V1}-X_{V2}}$ where t is between 0 and 1
4. Using t , the intersection vertex of edge is simply as follows:

- $X = X_{V1} + t * (X_{V1} - X_{V2})$
- $Y = Y_{V1} + t * (Y_{V1} - Y_{V2})$
- $Z = Z_{V1} + t * (Z_{V1} - Z_{V2})$

The final results are shown in figure8-(b)

5.1.2 Curve-fitting

In order to measure the circumference and area, a curve must be fitted through the resulting vertices so that its length can be recorded. Two approaches were tested to get an accurate curve:

- The first approach is polynomial interpolation. The main problem with this approach is that one or two polynomials are not enough to take all bends and ridges. Therefore, the section plane is divided into square regions and inside each square, the points are fitted into a cubic polynomial. This is known as cubic spline fitting and a sample plot is shown in figure 25 in the Annex. Due to the complexity of this approach, namely in joining all the cubic polynomials in one continuous and differentiable curve, and also due to the inability of cubic polynomials to capture small bends, another approach was used and is explained in point 2.
- The second approach is order the vertices in such a way that plotting them after ordering gives the shape of the circumference. The ordering algorithm goes as follows:
 1. All the vertices are sorted according to their Z value. Then, the point with highest Z is chosen and is appended to a matrix of ordered vertices.
 2. A frame originated at the chosen point is drawn as in figure 9-(a). Then, the following selection criteria is applied in order to determine the next vertex to be taken
 - (a) All the vertices that are within the fourth quadrant and have their Y and Z coordinates less than a certain threshold distance from the origin are taken. The threshold serves for faster execution and so that not all vertices of fourth quadrant are taken.
 - (b) From the chosen vertices, exclude all the ones that already exist in the ordered set.

- (c) If not empty, choose the vertex with the min distance to origin and append it to the ordered vertices and make it the new origin. Then repeat the same selection criteria.
3. The previous criteria keeps valid until it reaches the vertex shown in figure 9-(b) where there are no longer any vertices given by the previous selection criterion. If selected vertices are empty, the same selection criteria is repeated but with the third quadrant instead of the fourth. The latter reaches its end in figure 9-(c). Similarly, the selection criterion is changed to second quadrant then when empty, to the first quadrant as shown in figure 9-(d). It is worth noting that it doesn't necessarily end at the starting point because there are vertices are not always monotonous. For this reason, if the first quadrant selection criterion gives empty, it loops again through all the quadrants criteria and stops only if it loops through all the criteria and no vertex was appended.

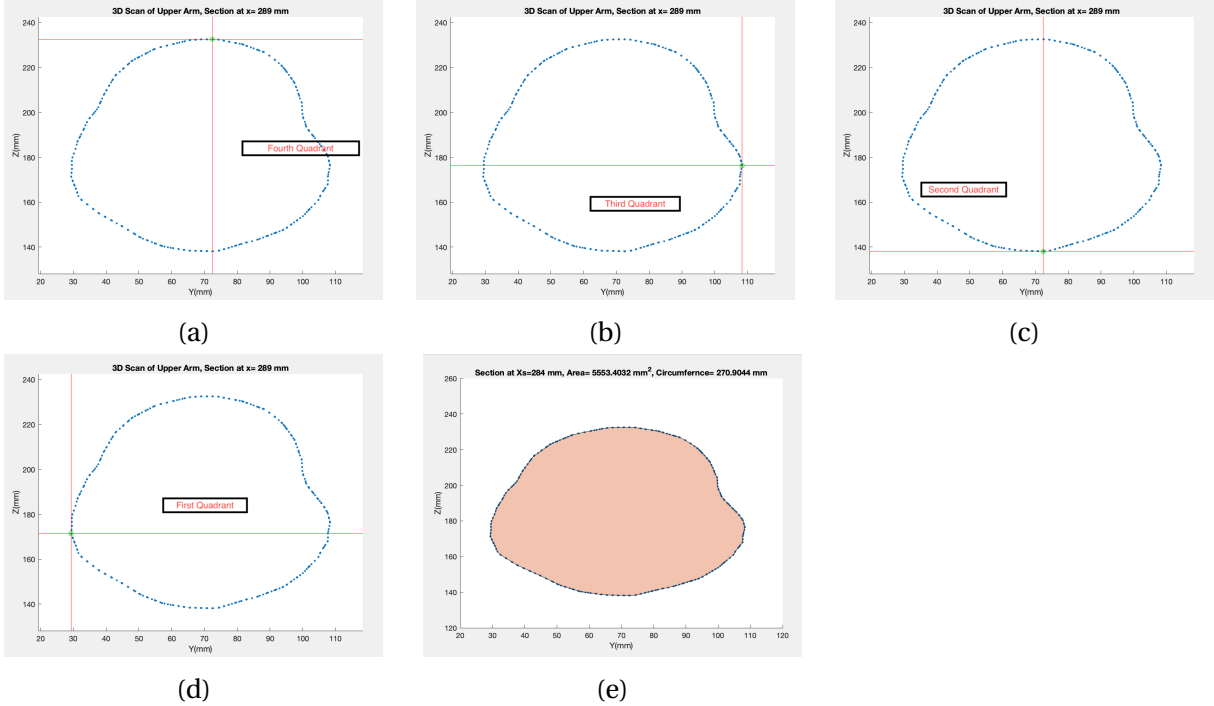


Figure 9: The figure shows the different steps for the ordering algorithm. Every loop keeps appending vertices in the direction of one quadrant until it finds none, then switches to the next quadrant in a clockwise manner. The loop keeps spinning until no new vertices are appended. Finally, after the ordering process, the built-in *polyarea* function can be applied to calculate the area of the section, where as the circumference is the summation of consecutive edges

As the vertices are now ordered, it is easy to plot the closed contour they for using the normal *plot* function , then by adding the distance between successive point, the circumference is obtained. Whereas the area is obtained using the built-in *polyarea* function which takes any set of ordered vertices and gives the area enclosed of the formed polygon as shown in figure 9-(e). However, it gives wrong results if two non-consecutive edges of the formed polygon intersect each other.

5.2 Validation with CAD Software

The circumference and area measurement algorithm was tested on 9 stretched arm samples. It is imperative to validate the MATLAB algorithm, and one way to do so is with a CAD software like SOLIDWORKS.



(a) A reference plane is constructed at a certain offset from elbow cut plane

(b) Removing the part of the arm within the offset using Extruded Cut. Area and perimeter are measured using Measure Tool

Figure 10: The scans are imported in CAD software to validate the circumference and area algorithm. Random section is taken for each of the 9 samples

Every *.stl* file is imported as a solid and a reference plane is drawn at the plane of the elbow cut. Then, by translating with a certain offset from the elbow, another reference plane is constructed. This is shown in figure 10-(a). Using the *Extruded Cut* feature, the part of the arm that lies within the offset is cut as shown in figure 10-(b). The Measure Tool in the evaluate tab gives the area and perimeter of section face. The results are tabulated in table 1.

Upper Arm Stretched Scans		SOLIDWORKS		MATLAB			
Sample #	Offset from elbow(mm)	perimeter (mm)	area(mm ²)	perimeter(mm)	area(mm ²)	perimeter relative error(%)	area relative error(%)
1	20	240.5	4448.3	240.5	4447.9	0	0.01
2	30	258.3	5075.5	258.3	5075.3	0	0
3	40	206.5	3340.7	206.5	3339.7	0.01	0.03
4	50	284.4	6241.5	284.3	6240.0	0.01	0.03
5	60	281.7	6229.6	281.7	6228.9	0.01	0.01
6	70	251.1	4828.8	251.1	4828.3	0.01	0.01
7	80	277.7	6109.7	277.7	6108.2	0.01	0.02
8	90	304.0	7288.1	303.9	7286.1	0.01	0.03
9	100	279.2	6083.9	279.2	6083.2	0.01	0.01
				MEAN ERROR		0.01	0.02
				STANDARD DEVIATION		0	0.01

Table 1: The circumference and area calculated with CAD software is compared to the results from the algorithm for 9 samples. The results indicate excellent estimation of the algorithm

A random offset was taken for each sample. The precision of the scanning apparatus is adjusted to 0.1 mm; therefore, all the measurements have 0.1 mm precision. The mean and standard deviation for the relative errors are nearly zero, which signifies an excellent estimation.

5.3 Robustness

It is worth noting that the mentioned algorithm applies for other body parts with different cross sections as shown below

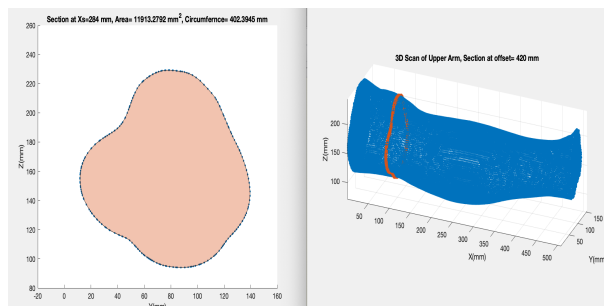


Figure 11: Circumference and Area Measurement Algorithm Tested on a Leg

6 Shoulder Identification for Stretched Arms

Determining the shoulder and elbow will be used down in section 8 where several muscle locations will be shown to be dependent on the elbow and shoulder locations. For the elbow, no easy was found to determine it without a marker; therefore, it was manually cut in the preliminary setup. To guarantee the consistency of cutting, all samples were cut with the same plane as shown in section 4.1. In what follows, an algorithm is explained to determine the shoulder.

6.1 Theoretical Framework and Scanning Guidelines

By referring to figure 12-(a) , it is seen that the shoulder joint is located at the humeral head, and figure 12-(b) shows that the humerus ends somewhere under the Deltoid muscle. The bulge of the Deltoid muscle is a prominent feature of a stretched arm of the arm as shown in figure 12-(c) . This feature can be determined in MATLAB, but although there is no way MATLAB can precisely predict the shoulder location without any markers, it is a good starting point to predict its proximity.

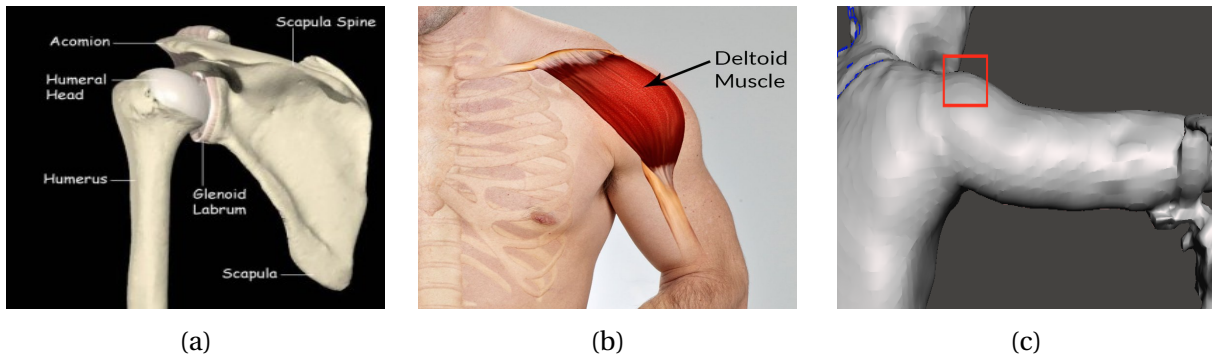
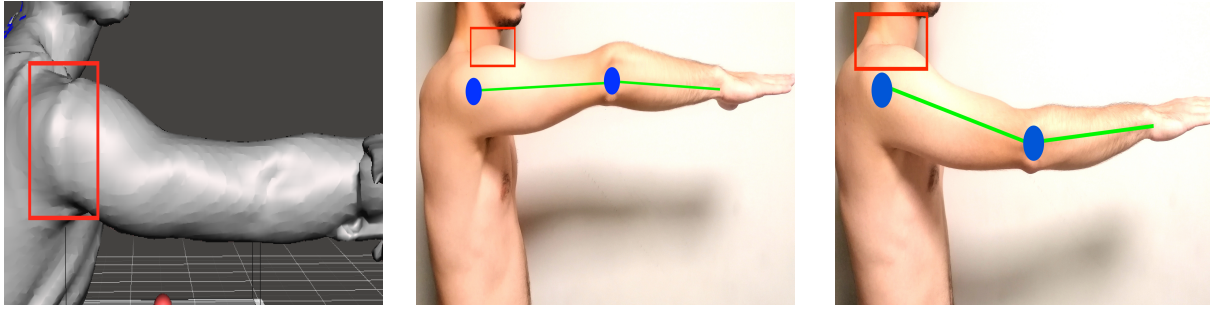


Figure 12: Approximation of Shoulder Joint Location Under the Deltoid Muscle Bulge

Nonetheless, certain limitations prevent the distinction the Deltoid bulge on all scans. Therefore, in what follows are recommended guidelines for easier shoulder identification:



(a) Clothing adds thickness near the Deltoid and prevents its distinction

(b) Deltoid bulge is clearer when the upper arm is as horizontal as possible

(c) When the upper arm is oblique, the bulge significantly disappears

Figure 13: Recommended guidelines that permit easy distinction of the Deltoid muscle bulge

- Remove all clothing around the shoulder area as they add a layer of thickness. This was the reason for disqualifying scans 2 and 4. An example is shown in figure 13-(a)
- For clearer distinction of the Deltoid bulge, the fore arm should be in line with the upper arm and making the arm as horizontal as possible as in figure 13-(b). This was seen in samples 3,7, and 8, and were therefore the scan where the bulge was most apparent. On the other side, if the upper arm is oblique downwards, the bulge becomes barely apparent as in figure 13-(c). This was the reason for disqualifying samples 5 and 9, but it was hardly captured for samples 1 and 6 even though their upper arms were oblique.
- It is also worth noting that the resolution of scans and the muscular state of the subjects could influence the bulging of the Deltoid muscle. Therefore, these guidelines could fail for some cases and hence, need to be tested on many subjects for verification

In the end, only samples 1,3,6,7,8 were chosen. Furthermore, to guarantee the consistency of the results that will follow, they were all aligned and cut at elbow with one plane as shown in section 4.1

6.2 MATLAB Algorithm

By looking at the right view of an arm, the extremum of the Deltoid muscle bulge is the vertex with the highest z-coordinate as shown in figure 14-(a). Then, the shoulder joint is approximated to be the center of gravity of the x-section at the extremum's x-coordinate. As for the

elbow, it is the center of gravity of the x-section at the max x coordinate of the cut. The elbow and shoulder joints are the yellow balls shown in figure 14.

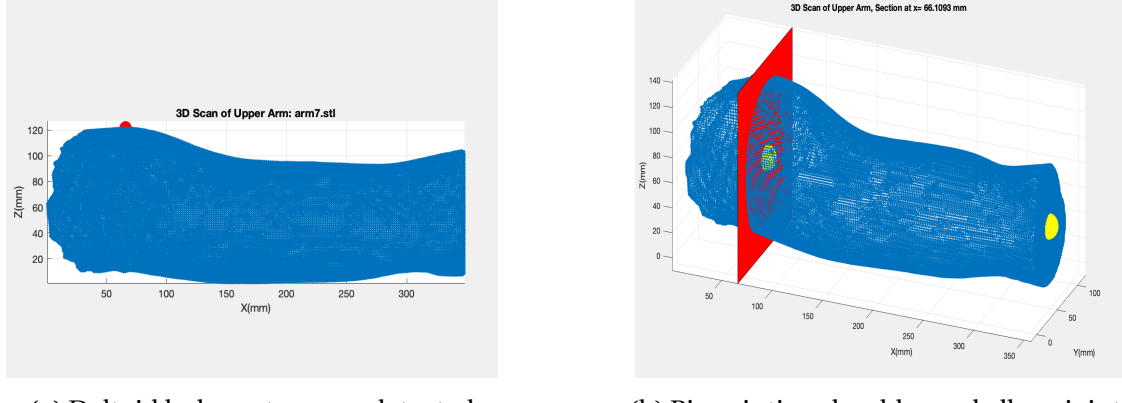


Figure 14: Approximating shoulder joint location by doing a section at the Deltoid bulge extremum

6.2.1 Humerus Length Comparison with Body Length

Assessing the quality of shoulder approximation can be achieved through performing a CT scan or a MRI or ultrasonic imaging. As these methods are out of reach for the author, another way is to see if the length of the humerus is more or less in line with a linear relationship with body length as proposed by [43] . Applying the above method enables to get an approximated humerus length for each sample as shown in figure 15. The study, done on 200 males and females from the northern district of Portugal, concluded a mean of 312.2 mm with a standard deviation of 20.51 mm . On the other side, the obtained results showed a mean of 262.8 mm with a standard deviation of 13.04 mm. Although the sample size is very small to draw any comparisons, it is a good sign that the results are coherent with the study in terms of linearity as shown in figure 15-(f).

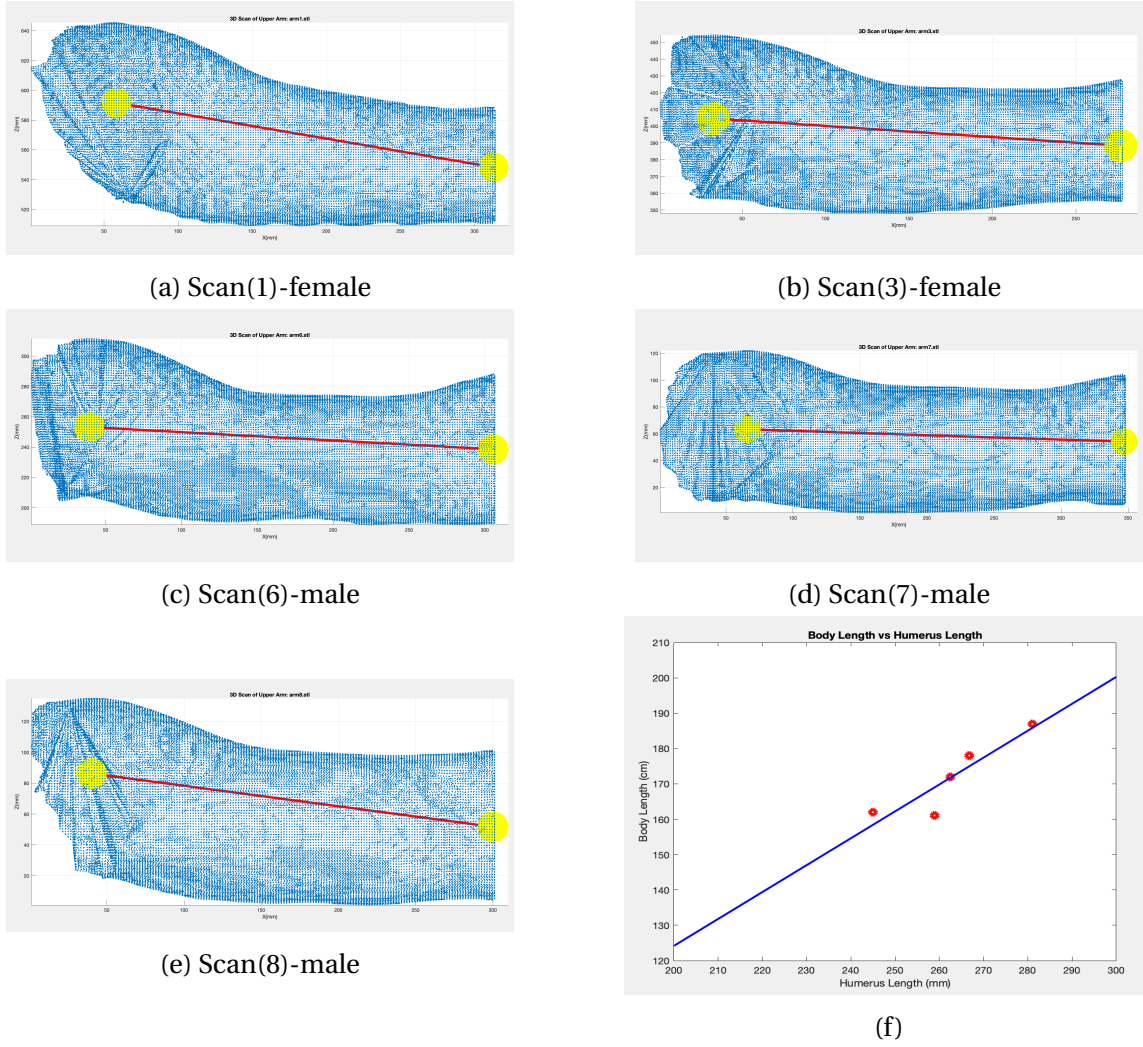


Figure 15: The shoulder joint location and elbow joint location was estimated by the algorithm explained in section 6.1. In figure (f), a linear relationship between the humerus length and length of the subject is found. This is in agreement with literature

7 Shoulder and Elbow Identification for Flexed Arms

7.1 Theoretical Framework

The same method used for the shoulder detection for the stretched arms is used for flexed arms, that is locating the extremum of Deltoid muscle bulge. And for the bulge to appear, the more horizontal the upper arm, the better appears.

As for the elbow, it can be seen by looking at the arm anatomy in figure 16 that the elbow joint is somewhere on the line joining the internal and external corners of flexion which are marked with red circles. Looking at figure 16, the elbow joint is closer to the external corner than it is to the internal one; therefore, it will be estimated to be 1/3 away from the external corner.

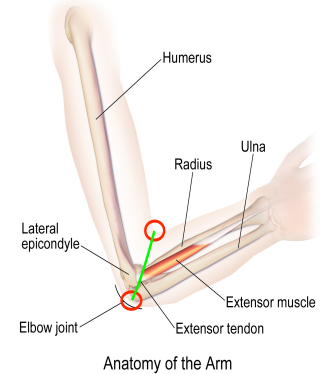


Figure 16: Elbow joint lies on the line joining the internal and external corners of arm flexion at approximately 1/3 from the external corner

7.2 MATLAB Algorithm

7.2.1 Shoulder Identification

The same way the shoulder is identified in the stretched arm scans hold for the flexed arms, but with a slight modification. Before, the highest vertex was identified as the extremum, but in this case, the highest vertex would be where the forearm cut ended. To solve this, the arm vertices are divided into two groups separated by the mid-value of the max and min x coordinates as shown in the figure 17. The extremum is chosen among the point of Group 1. Then, shoulder joint is approximated as explained in figure 14-(b)

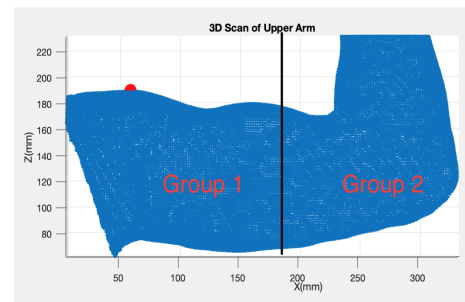
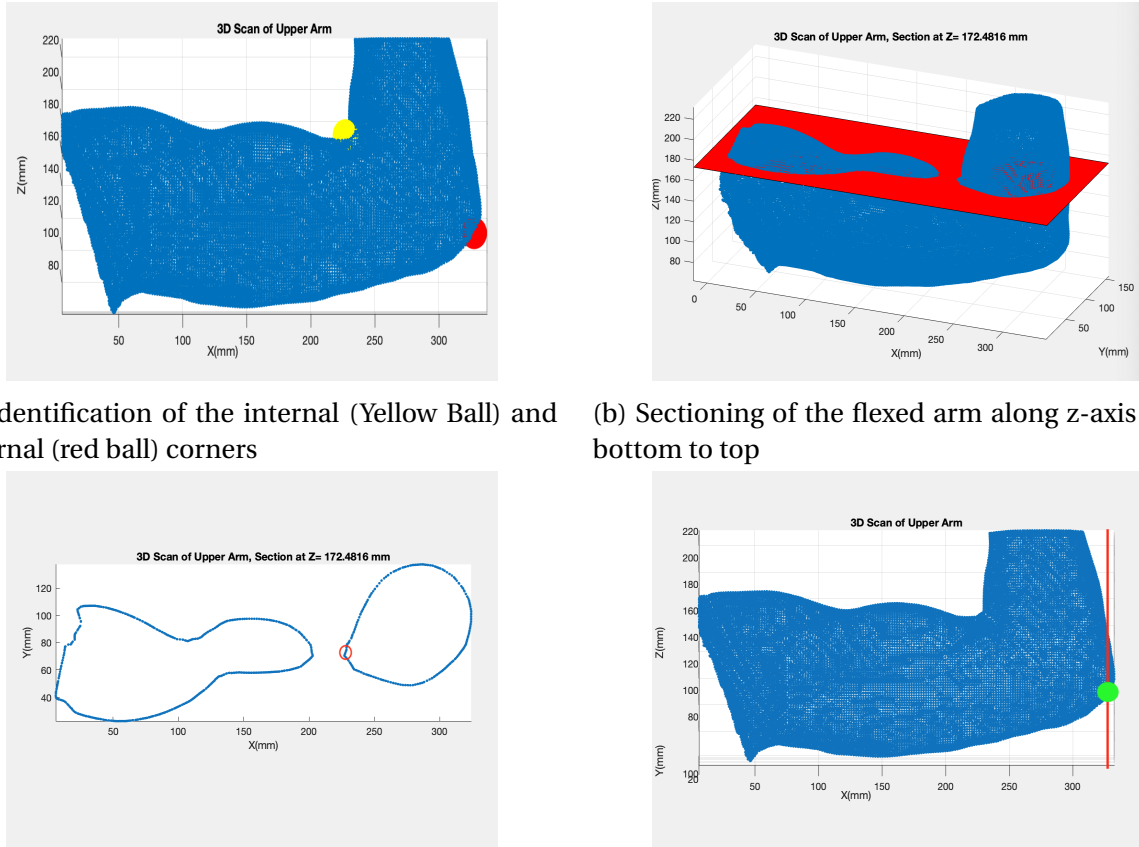


Figure 17: Vertices are divided into two groups depending on the mid-value of max and min x-coordinates. Then, Deltoid bulge extremum is chosen from among the vertices of Group 2

7.2.2 Elbow Identification

As stated in section 7.1, the elbow joint approximation is based upon identifying the line joining the external and internal corners of the the flexed arm as in figure 18-(a).



(c) Section points are sorted in x- direction. Internal corner is spotted by comparing the x-difference for each two consecutive points

(d) External corner is determined as the lowest point of an x-section 1 cm away far from max x-coordiante

Figure 18: Elbow joint estimation using the line joining the internal and external corners of a flexed arm

1. Internal Corner:

This algorithm takes advantage of the concavity between the belly of the biceps muscle and the flexed forearm to determine the proximity of the internal corner. The steps are as follows:

- Sections are taken along the Z-axis as in figure 18-(b) from bottom to top
- Each resulting set of section vertices is sorted according to their x values in ascend-

ing order

- Each two consecutive points are compared and if a difference of more than 1 cm is spotted between the two points, then the second point is recorded as in figure 18-(c) and the sectioning stops. This point is regarded as the internal corner.

2. External Corner:

- The external corner is determined by making a section along x-axis at an offset of 1 cm from the point with highest x-coordinate
- From the section points, the point with the lowest z-coordinate is regarded as the external corner as in figure 18-(d). For this reason, it is imperative that the forearm is slightly flexed to the side of the upper arm.

Finally, correlating with section 6.2.1, the following results are obtained:

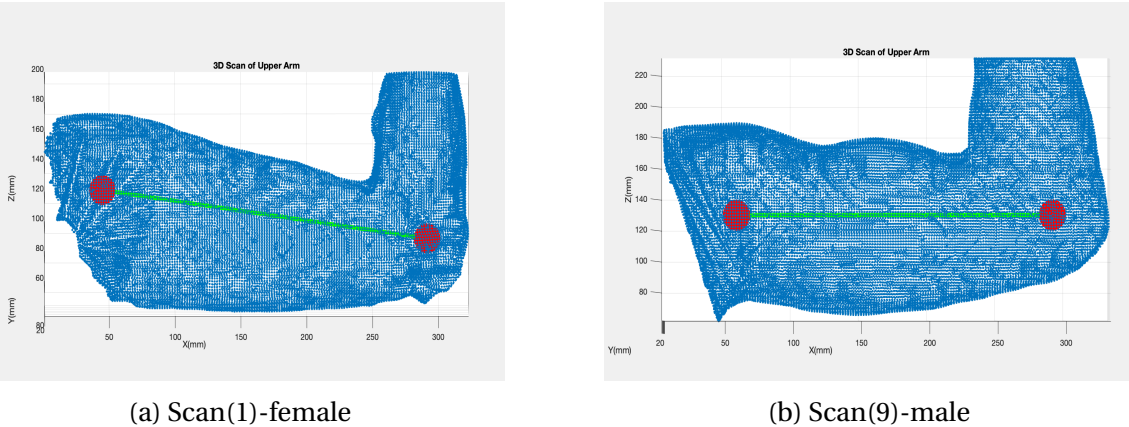


Figure 19: The shoulder joint location and elbow joint location was estimated by the algorithm explained in section 7.1. This gives an estimation for the humerus length. The humerus length for sample 1 stretched arm is less than 1 cm close to sample 1 flexed arm

The two flexed arm scans are in fact for samples 1 and 9 from of the stretched arm scans. It is interesting to compare the obtained humerus length from both scans for each sample. Unfortunately, scan 9 in the stretched arms was not among the chosen scans for shoulder identification but scan 1 was. For stretched arm scan, sample 1 recorded a humerus length of *25.9 cm* compared to *25.2 cm* for the flexed scan.

8 Benchmarking: Biceps Brachii Identification

One of the goals of the study is to be able to pinpoint certain landmarks on the upper arm that are used for sensor placement like EMG sensors. Referring to the SENIAM(Surface ElectroMyoGraphy for the Non-Invasive Assessment of Muscles) project [46], it gives guidelines for the EMG electrodes placement on some upper arm muscles, namely the Biceps Brachii and Triceps Brachii , as shown in figures 20-(a) and 20-(b). For the scope of this study, the biceps muscle is easier to determine than triceps muscle given the posture of the arm scans in hand.

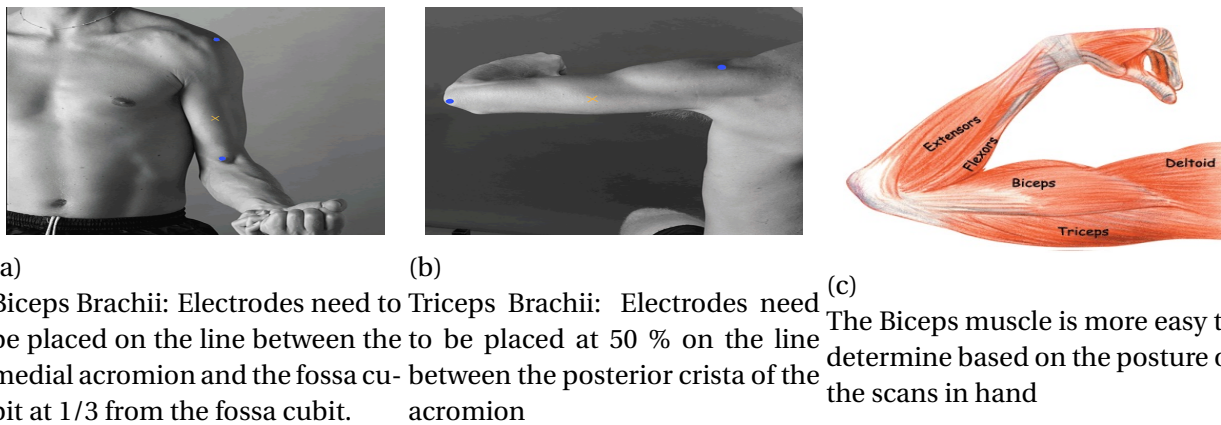


Figure 20: SENIAM Recommendations for EMG electrode placement: benchmarking on biceps brachii

Although the reference points from the SENIAM recommendation for the Biceps Brachii are not exactly the determined points in the previous sections, they are definitely in their proximity. Therefore an empirically modified standard was followed to determine the biceps brachii on the processed scans in the previous sections. The standard is:

On the line joining the approximated shoulder and elbow joints, the biceps brachii is 2/5 away from the elbow

The biceps brachii identification is easier done on flexed arms, because the biceps bulge when the forearm is flexed. Essentially, after going 2/5 away from the elbow, an x section is done and the biceps brachii proximity is recorded as the point with highest z, that due to the fact of the bulging belly the biceps form. Finally, obtained results shown below:

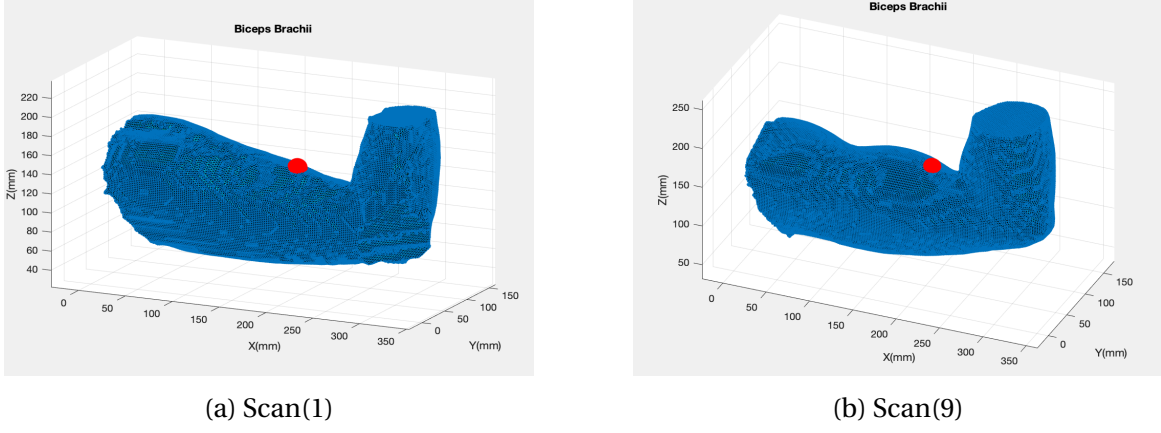


Figure 21: Biceps Brachii Identification for Flexed Arm Scans

9 Conclusions and Future Work

Starting with the circumference and area measurement, the algorithm succeeded in giving excellent estimations. Furthermore, the developed algorithm is robust because it can be used on various body parts. It can also be used to extract the max perimeter or area of a body part, or to compare the contours of the same sections on different positions, for example testing the how the circumference of a knee section changes during the Gait cycle. On the other side, one misaligned point that does not come in the right order gives wrong results. Further testing should be done on multiple geometries to see how reliable the algorithm is.

Moving to the shoulder approximation for the stretched scan, although it is not accurate, it is a good starting point to finally see a linear relation between the humerus length and the body length. The difference between the mean from the study[43] and the one from this study is because the shoulder joint location is an approximation , and because the plotted length is the Euclidean distance between two points whereas the actual humerus is a bit deformed, so it isn't entirely correct to approximate it with a Euclidean distance.

As for the EMG sensors benchmarking on Biceps Brachii, the algorithm was able to determine at least a point on the biceps muscle for the two scans. This is apparent because the identified point lies on the belly of the biceps muscle. This opens future work for embedding those

identified points into an upper arm exoskeleton cuff. This will be a first iteration of a data-driven design process

In the end, it is worth noting that this algorithm can be developed for any type of sensorized interface, and it was only benchmarked on EMG sensors to prove its usability.

10 Annex

10.1 Right Views of All Stretched Arm Scans

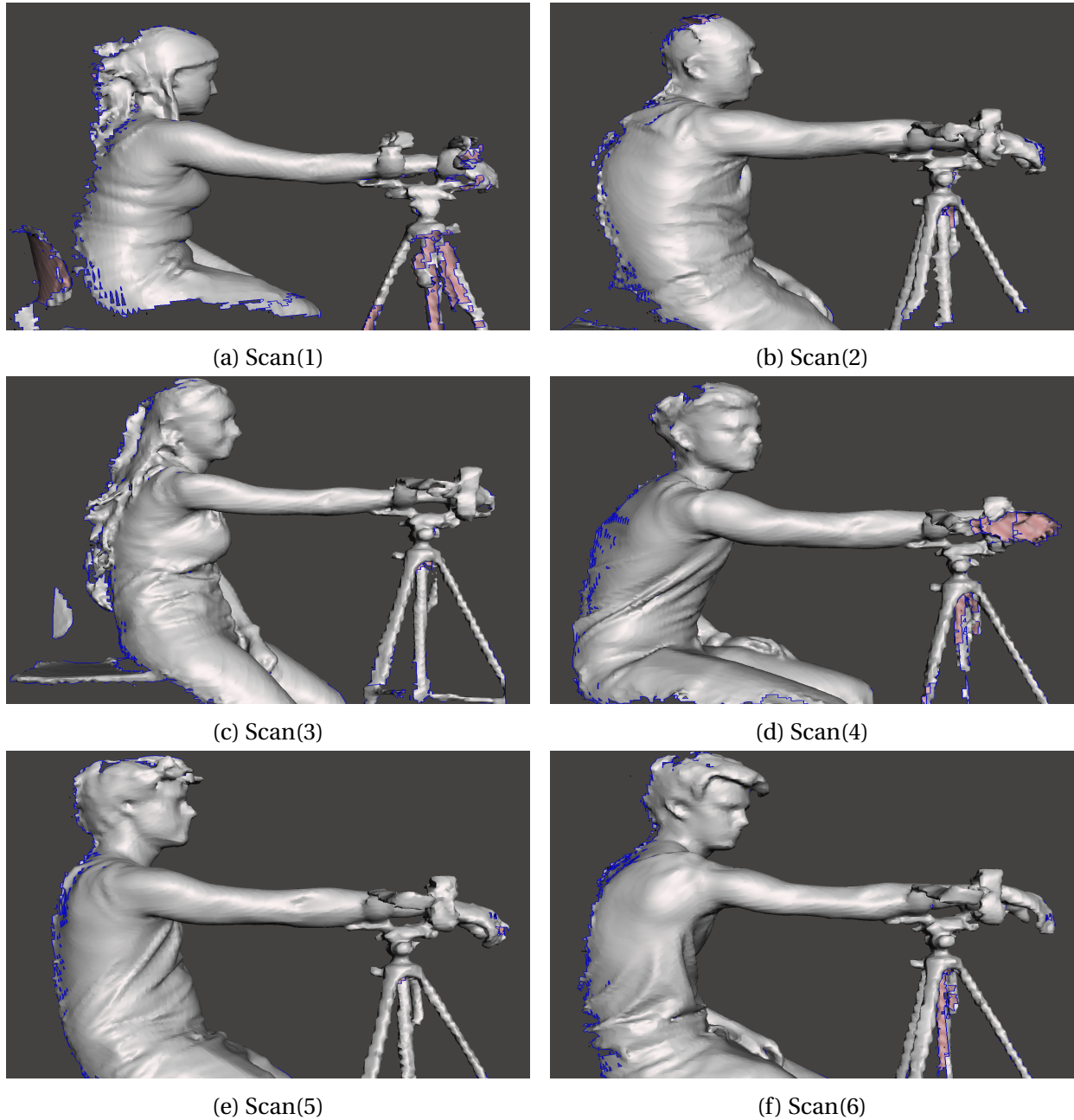


Figure 22: Right Views of All Stretched Arm Scans

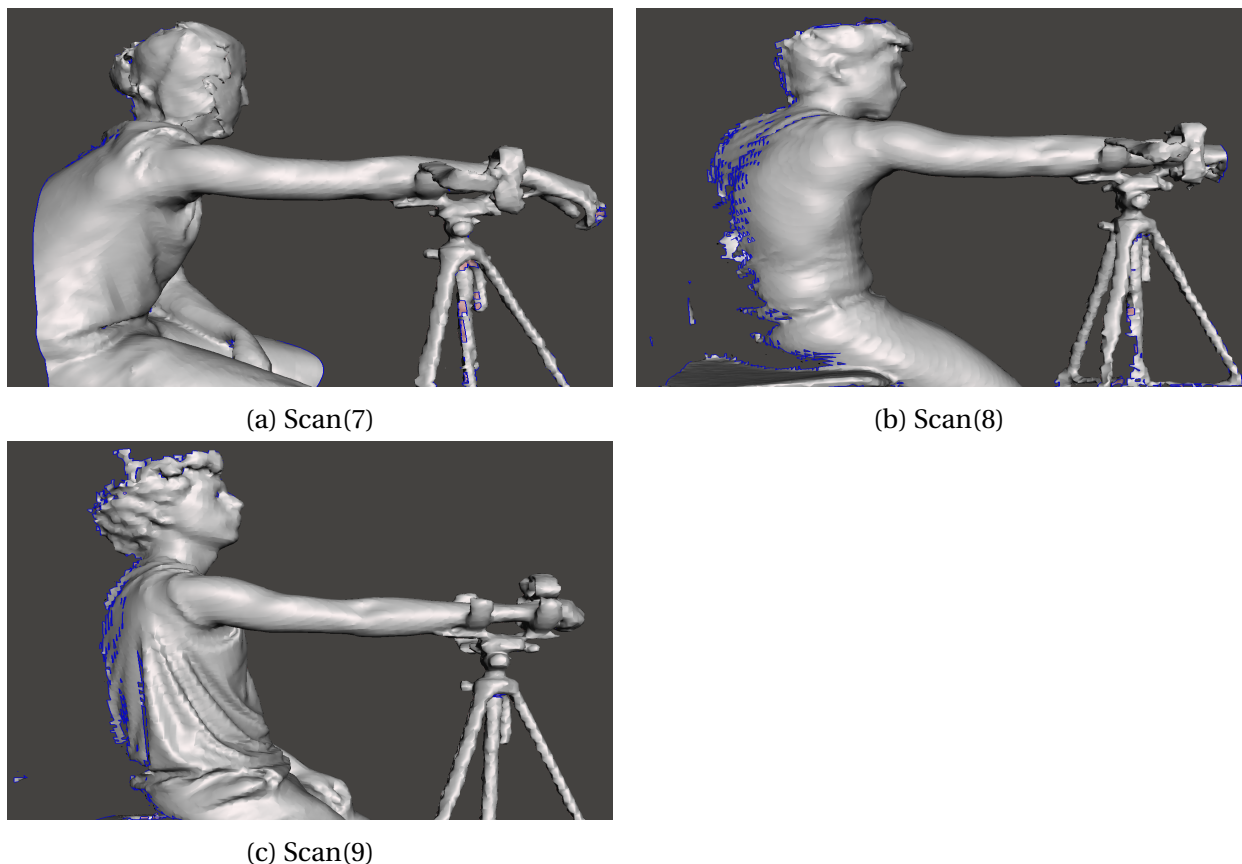


Figure 23: Right Views of All Stretched Arm Scans-Continued

10.2 Right Views of All Flexed Arm Scans

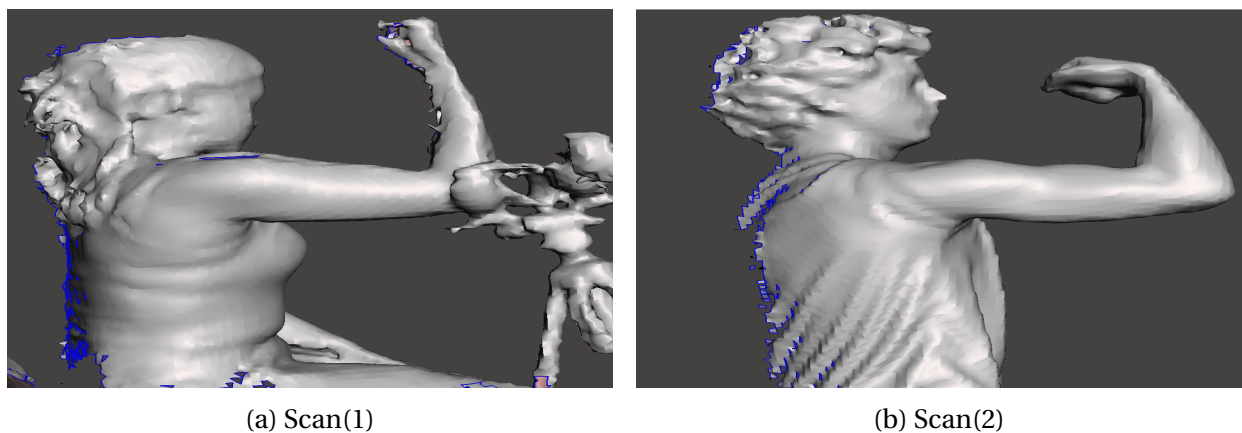


Figure 24: Right Views of All Flexed Arm Scans

10.3 Cubic Spline Fitting Method

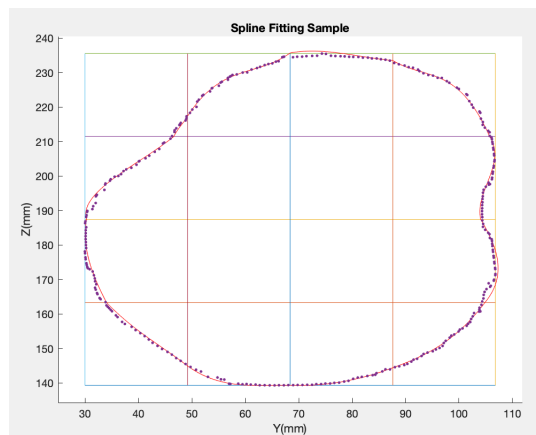


Figure 25: Cubic Spline Fitting Method

11 Bibliography

- 1 A. J. Young and D. P. Ferris, "State of the art and future directions for lower limb robotic exoskeletons," *IEEE Trans. Neural Syst. Rehabil. Eng.*, vol. 25, no. 2, pp. 171–182, 2017.
- 2 World Health Organization, Regional Office for Europe [Internet]. [cited 1 March 2021]. Available from: <https://www.euro.who.int/en/health-topics/Life-stages/disability-and-rehabilitation/d-and-statistics/facts-on-rehabilitation>.
- 3 A. Wege and A. Zimmermann, "Electromyography sensor based control for a hand exoskeleton," 2007 IEEE International Conference on Robotics and Biomimetics (ROBIO), Sanya, China, 2007, pp. 1470-1475, doi: 10.1109/ROBIO.2007.4522381.
- 4 Bryce T, Dijkers M, Kozlowski A. Framework for Assessment of the Usability of Lower-Extremity Robotic Exoskeletal Orthoses. *Am J Phys Med Rehabil.* 2015 and DOI:10.1097/PHM.0000000000000000 94(11):1000-1014.
- 5 <http://www.suitx.com/phoenix>, Phoenix | suitX [Internet]. Suitx.com.[cited 1 March 2021]. Available form:.
- 6 CYBERDYNE [Internet]. [cited 1 March 2021]. Available from: <https://www.cyberdyne.jp/english/product/>

- 7 <https://eksobionics.com/eksoue/>?, eksobIONICS.[Internet].[cited 1 March 2021]. Available from:.
- 8 Asbeck A. T., De Rossi S. M. M., Holt K. G., and Walsh C. J., "A biologically inspired soft exosuit for walking assistance," *The International Journal of Robotics Research*, vol. 34, no. 6, pp. 744–762, May 2015,.
- 9 Yandell M. B., Quinlivan B. T., Popov D., Walsh C., and Zelik K. E., "Physical interface dynamics alter how robotic exosuits augment human movement: implications for optimizing wearable assistive devices," *Journal of NeuroEngineering and Rehabilitation*, v.
- 10 Yandell MB, Ziemnicki DM, McDonald KA, Zelik KE (2020) Characterizing the comfort limits of forces applied to the shoulders, thigh and shank to inform exosuit design. *PLoS ONE* 15(2): e0228536. <https://doi.org/10.1371/journal.pone.0228536>.
- 11 S. M. M. de Rossi et al., "Sensing pressure distribution on a lower-limb exoskeleton physical human-machine interface," *Sensors*, vol. 11, no. 1, pp. 207–227, 2011.
- 12 Tamez-Duque, Jesús Cobian-Ugalde, Rebeca Kilicarslan, Atilla Venkatakrishnan, Anusha Soto, Rogelio Contreras-Vidal, José. (2015). Real-Time Strap Pressure Sensor System for Powered Exoskeletons. *Sensors* (Basel, Switzerland). 15. 4550-63. 10.3390.
- 13 Michael Wehner (2012). Man to Machine, Applications in Electromyography, EMG Methods for Evaluating.
- 14 R. Merletti, *Electromyography: physiology, Engineering and noninvasive applications*. Piscataway, NJ, 2010.
- 15 Yogeswaran Ganesan, Suresh Gobee, Vickneswary Durairajah," Development of an Upper Limb Exoskeleton for Rehabilitation with" , 2015 IEEE International Symposium on Robotics and Intelligent Sensors (IRIS 2015).
- 16 F. Hardalaç and R. Canal, "EMG circuit design and AR analysis of EMG signs," *J. Med. Syst.*, vol. 28, no. 6, pp. 633–642, 2004.

- 17 M. Asghari Oskoei and H. Hu, "Myoelectric control systems-A survey," *Biomed. Signal Process. Control*, vol. 2, no. 4, p. 2007, 2007.
- 18 K. Kiguchi and Y. Hayashi, "An EMG-Based Control for an Upper-Limb," *IEEE Trans. Syst. Man, Cybern. Part B Cybern.*, vol. 42, no. 4, pp. 1064–1071, 2012.
- 19 S. M. M. de Rossi et al., "Sensing pressure distribution on a lower-limb exoskeleton physical human-machine interface," *Sensors*, vol. 11, no. 1, pp. 207–227, 2011.
- 20 www.seniam.org, SENIAM.[Internet]. Available form:.
- 21 Bernard Grundlehner, Vojkan Mihajlović,Ambulatory EEG Monitoring,Editor(s): Roger Narayan,Encyclopedia of Biomedical Engineering,Elsevier,2019,Pages 223-239,ISBN 9780128051443,<http://0-12-801238-3.10885-2>.
- 22 <http://www.rehab-robotics.com.hk/hoh/index.html>, Rehab-Robotics.[Internet].[cited 2 March 2021].Available from:.
- 23 Cláudia Teixeira Espadinha, " Integration of 3D printed sensors into orthotic devices", Vrije Universiteit Brussel,2020. [24] <https://www.seeedstudio.com/blog/2019/12/27/what-is-emg-sensor-myoware-and-how-to-use-with-arduino/>, Seedstudio. [Internet].[cited 1 March 2021]. Available from:.
- 25 <https://mfimedical.com/products/ambu-neuroline-monopolar-emg-needle-electrode>, MFIMedical. [Internet].[cited 1 March 2021]. Available from:.
- 26 J. D. E. Luca, M. Knaflitz, C. J. De, and L. Myoelectric, "Myoelectric manifestations of fatigue in voluntary and electrically elicited contractions," 2018.
- 28 Conrad, Kendon J., et al.
- 29 G. Wolterink, R. Sanders, and G. Krijnen, "Towards 3D-Printing of soft sEMG sensing structures," pp. 1–2, 2017.
- 30 Moltedo, Marta Bacek, Tomislav Serrien, Ben Langlois, Kevin Vanderborght, Bram Lefever, Dirk Rodriguez-Guerrero, Carlos. (2020). Walking with a powered ankle-foot orthosis: the effects of actuation timing and stiffness level on healthy users.

- 31 www.sciencedirect.com, [Internet].[cited 2 March 2021]. Available from:.
- 40 www.muscleandmotion.com shouler anaytomy ref
- 41 shoulder muscles 2 https://www.kenhub.com/en/library/anatomy/shoulder-muscles
- 43 AMERICAN JOURNAL OF PHYSICAL ANTHROPOLOGY 112:39–48 (2000)
- 44 https://www.liebscher-bracht.com/en/encyclopedia-of-pain/shoulder-impingement/
- 45 https://www.sportsmd.com/sports-injuries/shoulder-injuries/deltoid-strain/
- 46 https://seniam.org/